Mg^{2+} Block Unmasks Ca^{2+}/Ba^{2+} Selectivity of α1G T-Type Calcium Channels

Jose R. Serrano,* Shervin R. Dashti,* Edward Perez-Reyes,† and Stephen W. Jones*

*Department of Physiology and Biophysics, Case Western Reserve University, Cleveland, Ohio 44106; and †Department of Pharmacology, University of Virginia, Charlottesville, Virginia 22908 USA

ABSTRACT We have examined permeation by Ca^{2+} and Ba^{2+}, and block by Mg^{2+}, using whole-cell recordings from α1G T-type calcium channels stably expressed in HEK 293 cells. Without Mg_o^{2+}, inward currents were comparable with Ca^{2+} and Ba^{2+}. Surprisingly, three other results indicate that α1G is actually selective for Ca^{2+} over Ba^{2+}. 1) Mg^{2+} block is ~7-fold more potent with Ba^{2+} than with Ca^{2+}. With near-physiological (1 mM) Mg_o^{2+}, inward currents were ~3-fold larger with 2 mM Ca^{2+} than with 2 mM Ba^{2+}. The stronger competition between Ca^{2+} and Mg^{2+} implies that Ca^{2+} binds more tightly than Ba^{2+}. 2) Outward currents (carried by Na^+) are blocked more strongly by Ca^{2+} than by Ba^{2+}. 3) The reversal potential is more positive with Ca^{2+} than with Ba^{2+}, thus $P_{Ca} > P_{Ba}$. We conclude that α1G can distinguish Ca^{2+} from Ba^{2+}, despite the similar inward currents in the absence of Mg_o^{2+}. Our results can be explained by a 2-site, 3-barrier model if Ca^{2+} enters the pore 2-fold more easily than Ba^{2+} but exits the pore at a 2-fold lower rate.

INTRODUCTION

Ca^{2+} entry through voltage-dependent calcium channels is critical for both electrical and chemical signaling. To perform such functions, calcium channels must select for Ca^{2+} over more plentiful monovalent cations. The basic mechanism for Ca^{2+} selectivity is not simple molecular sieving, because calcium channels pass large monovalent cations if divalent cations are absent (McCleskey and Almers, 1985). Selectivity involves ion-ion interactions (Almers and McCleskey, 1984; Hess and Tsien, 1984; Dang and McCleskey, 1998) and electrostatic interactions of ions with negatively charged amino acids in the channel pore (Yang et al., 1993; Nonner and Eisenberg, 1998).

Permeation mechanisms have been studied most thoroughly for L-type calcium channels. Many of the basic features are also present in T-type Ca^{2+} channels, including high permeability to monovalent cations and block by micromolar concentrations of divalent cations (Fukushima and Hagiwara, 1985; Lux et al., 1990), but there are also differences in ion selectivity among calcium channels. Notably, inward currents are ~2-fold larger with Ba^{2+} than Ca^{2+} for L-channels (Hess and Tsien, 1984), but most T-channels show comparable inward currents with Ca^{2+} or Ba^{2+} (Fukushima and Hagiwara, 1985; Bean, 1985; Carbone and Lux, 1987; Huguenard, 1996).

The recent cloning and functional expression of T-type calcium channels allows the study of their biophysical properties in isolation (Perez-Reyes et al., 1998). We recently examined the gating kinetics of the α1G channel (Serrano et al., 1999), which is highly expressed in many brain regions, including thalamic relay neurons (Talley et al., 1999), where T-channels play an important role in generation of bursting activity (Huguenard, 1996). In our initial experiments on the ion selectivity of α1G, we were surprised to find that inward currents were much larger with Ca^{2+} than with Ba^{2+} (Dashti et al., 1999). We report here that this results from preferential block by Mg^{2+} of currents carried by Ba^{2+}. Without Mg^{2+}, inward currents are very similar with Ca^{2+} and Ba^{2+}. However, the reversal potential (V_R) is more positive, and outward monovalent currents are smaller with Ca^{2+}, indicating Ca^{2+} selectivity. We conclude that α1G can distinguish Ca^{2+} from Ba^{2+} ions. Our results can be described by Eyring rate theory (a 2-site, 3-barrier model) if Ca^{2+} enters the pore more easily than Ba^{2+}, but Ba^{2+} exits more rapidly. Small differences between the energetics of Ca^{2+} versus Ba^{2+} are sufficient to produce a ~7-fold difference in Mg^{2+} block, although inward currents carried by Ca^{2+} and Ba^{2+} are similar over a wide voltage range.

MATERIALS AND METHODS

Electrophysiology

Whole-cell recordings were made from the Nr2+ cell line, HEK 293 cells stably transfected with rat α1G (Lee et al., 1999a), as described previously (Serrano et al., 1999). Briefly, data were recorded at room temperature using Clampex (pClamp 6.03, Axon Instruments, Foster City, CA) with an Axopatch 200A amplifier. Data were usually sampled at 20 kHz following 10 kHz analog filtering. Series resistances (initially 6.6 ± 0.4 MΩ, $n = 34$) were compensated nominally by 80–90%.

The standard intracellular (pipette) solution contained 140 mM NaCl, 2 mM $CaCl_2$, 11 mM EGTA, 10 mM HEPES, 4 MgATP, pH 7.2 with ~25 mM NaOH. Free $[Ca^{2+}]_i$ was 40 nM, and free $[Mg^{2+}]_i$ was 0.8 mM, calculated from the program Bound and Determined (BAD) (Brooks and Storey, 1992). The extracellular solutions contained 140 mM NaCl, 2 mM $CaCl_2$ or $BaCl_2$ (as noted), 0 or 1 mM $MgCl_2$ (as noted), 10 mM HEPES, pH 7.2 with ~5 mM NaOH.

Extracellular solutions were exchanged by a gravity-driven flow system, remotely controlled by solenoid valves. We found it difficult to record from cells with sufficient stability to obtain fully reversible responses

Received for publication 22 June 2000 and in final form 11 September 2000.

Address reprint requests to Dr. Stephen W. Jones, Dept. of Physiology and Biophysics, Case Western Reserve University, Cleveland, OH 44106. Tel.: 216-368-5527; Fax: 216-368-3952; E-mail: swj@po.cwru.edu.

0006-3495/00/12/3052/11 $2.00

(requiring >10 min), resulting from slow changes in leakage currents, current amplitudes, etc. Thus, many comparisons of currents in different conditions were made between populations of cells (e.g., part *B*, Figs. 1–6), but key results were confirmed in cells where reversible effects were obtained (as illustrated in part *A*, Figs. 2–5). Some averaged *I-V* curves are shown in multiple figures, to make pairwise comparisons between different conditions.

Data analysis

Currents were analyzed using Clampfit v.6 and Microsoft Excel (v.5 or 97), and graphs were prepared using Microcal Origin v.5 and Micrografx Designer v.7. Unless noted, values are given as mean ± SEM. For averaged data in the figures, error bars are shown if larger than the symbols. Current records in the figures were Gaussian-filtered 2 kHz (unless noted otherwise) using Clampfit. Statistical significance levels given in the text are from unpaired 2-tailed *t*-tests (Excel), with $p < 0.05$ considered to be significant.

Our experiments require accurate voltage clamp to control the large currents observed over a wide voltage range. For analysis of instantaneous *I-V* relations, cells were selected based on two primary criteria, the rise time of tail currents at −100 mV, and the effect of partial inactivation on the time course of tail currents at −100 mV (protocol illustrated in Fig. 7). For selected cells, ~70% inactivation affected the time constant for channel deactivation by <20% (corresponding to 5 mV or less of series resistance error, given the voltage-dependence of channel closing; Serrano et al., 1999).

Instantaneous *I-V* relations were measured by fitting single exponentials to the decay of current following a brief (2-ms) step to +60 mV (see Fig. 1 *A*). The exponential fit began when the tail currents reached a peak (0.3–0.7 ms), and extended to the end of the 40-ms voltage steps. In some cells, the tail currents were well described by a single exponential over that entire time course, while other cells exhibited slight deviations from exponential decay during the first ~1 ms (which was not strongly weighted in the fit). The amplitude of the fitted exponential at the starting point of the fit was used for the instantaneous *I-V* measurements shown, as an estimate of the current at the time when accurate voltage clamp was actually achieved (extrapolating back to time 0 would overestimate the tail current amplitudes at extreme voltages). This procedure resulted from much trial-and-error, and was judged to give more consistent results than alternative approaches (e.g., measurement of the actual peak tail current, which was more sensitive to filtering and to slight deviations from exponential kinetics). However, different methods produced only subtle differences in the *I-V* relations, as the main results were visible "by eye" in the raw currents (see part *A*, Figs. 1–5).

Calculations and models

For two permeant ions A and B of any charge (z_A, z_B), each of which may be present on both sides of the membrane, the Goldman-Hodgkin-Katz permeability ratio (P_A/P_B) was calculated from the observed reversal potential (V_R) (Frazier et al., 2000):

$$P_A/P_B = \frac{-z_B^2([B]_i - [B]_o\, e^{-\nu_B})(1 - e^{-\nu_A})}{z_A^2([A]_i - [A]_o\, e^{-\nu_A})(1 - e^{-\nu_B})} \quad (1)$$

where $\nu_A = z_A V_R F/RT$ and $\nu_B = z_B V_R F/RT$. Permeability ratios in the Results were calculated using concentrations, not activities.

The voltage dependence of Mg^{2+} block was described by a simplified Woodhull (1973) model, assuming that Mg^{2+} binds to a single site within the pore, can enter the pore only from the outside, and cannot permeate:

$$f = 1/\{1 + [Mg^{2+}]/(K_{D,0}e^{z\delta FV/RT})\} \quad (2)$$

where f is the fraction of current remaining unblocked in the presence of Mg^{2+}, $K_{D,0}$ is the dissociation constant for Mg^{2+} at 0 mV, $z = 2$ is the charge on Mg^{2+}, and δ is the apparent electrical location of the binding site, as a fraction of the electrical field of the membrane measured from the outside.

Permeation and Mg^{2+} block were also described by a 2-site, 3-barrier model including ion-ion repulsion, based on the model of Almers and McCleskey (1984). Specifically, positions of the barriers in the electrical field (δ values) were 0.05, 0.5, and 0.95, with wells at 0.33 and 0.67. Each rate constant (k) was related to barrier/well energies by:

$$k = k_0\, e^{-\Delta Gz\Delta\delta FV/RT} \quad (3)$$

where ΔG is the difference in zero-voltage energies between the well and the barrier, z is the charge on the ion, and $\Delta\delta$ is the difference in electrical locations. For comparison to most previous models, we use kT/h (6.1×10^{12}) as the preexponential factor (k_0) for all rate constants, including entry of ions into the pore. This has been criticized (Nonner and Eisenberg, 1998), especially for entry rates (Yue and Marban, 1990), so the height of the "energy barriers" in the model should not be interpreted literally (Andersen, 1999). When both binding sites were occupied, rate constants for exit from the pore were increased by the factor $Q \cdot z_A \cdot z_B$, where $Q = 11.89$ and z_A and z_B are the charges on the ions in the two sites (Almers and McCleskey, 1984). The model was implemented using the SCoP simulation package (v.3.51; Simulation Resources, Berrien Springs, MI). Whole-cell currents were scaled to typical single-channel current levels assuming 8000 channels per cell. The energy levels of the barriers and wells were varied for each ion (Ca^{2+}, Ba^{2+}, Mg^{2+}, and Na^+). To limit the number of free parameters, the energy profiles were assumed to be symmetrical for Ca^{2+}, Ba^{2+}, and Na^+ (but *not* Mg^{2+}), and the middle barrier was the same height (with respect to the outer well) for all ions. External barriers were constrained to be from 8 to 12 *RT*, and the outer well for Mg^{2+} was constrained to be at least 1 *RT* less than the outer barrier. The 11 resulting parameters (2 energies each for Ca^{2+}, Ba^{2+}, and Na^+, and 5 for Mg^{2+}) were estimated using the SCoPfit program, which uses the principal axis (Praxis) algorithm.

RESULTS

With Mg_o^{2+}, inward currents are larger with Ca^{2+} than with Ba^{2+}

To examine the ion selectivity of the α1G channel, we began with nearly normal ionic conditions, including 2 mM Ca_o^{2+}, except that K_i^+ was replaced by Na_i^+. The recording solutions contained 1 mM Mg_o^{2+} and an estimated 0.8 mM free Mg_i^{2+} (see Materials and Methods). To examine permeation using whole-cell currents, we measured instantaneous current-voltage (*I-V*) relations following brief, strong depolarizations designed to activate channels while producing minimal inactivation (Fig. 1). In principle, each prepulse should activate the same number of channels, producing the same outward current at +60 mV during each 2-ms step. If so, the currents measured shortly after repolarization should reflect the voltage-dependence of current flow through a constant number of open channels (Hodgkin and Huxley, 1952). This analysis is aided by the characteristically slow deactivation of T-channels, with $\tau > 1$ ms even at −120 mV (Serrano et al., 1999).

With 2 mM Ca^{2+}, the reversal potential (V_R) was +26.0 ± 2.0 ($n = 8$), in good agreement with our previous

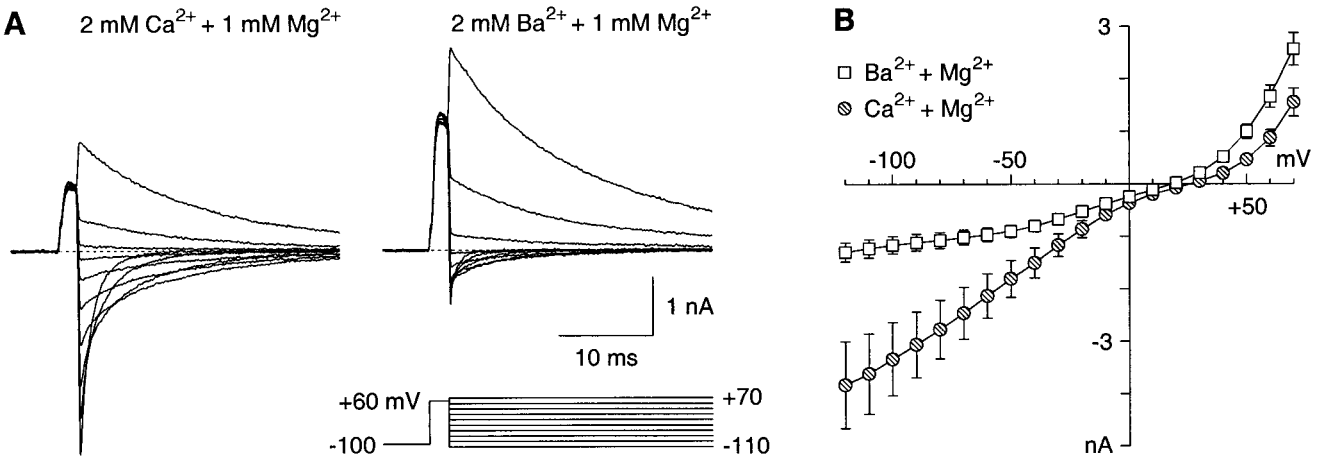

FIGURE 1 With Mg_o^{2+}, inward currents are larger with Ca^{2+} than with Ba^{2+}. (*A*) Sample records from the protocol used to measure instantaneous *I-V* relations, in Ca^{2+} (*left*) or Ba^{2+} (*right*). Note small inward currents and large outward currents with Ba^{2+}. Channels were activated by a 2-ms step to +60 mV, immediately followed by voltage steps in 10-mV increments from −120 to +70 mV; every other voltage step is illustrated here. The decay of currents at each voltage reflects a combination of channel closing (deactivation) and inactivation (Serrano et al., 1999); cell a9n26 (Ca^{2+} + Mg^{2+}); cell c9711 (Ba^{2+} + Mg^{2+}). (*B*) Instantaneous *I-V* relations, measured as described in Materials and Methods, from the protocol of *A*, averaged from 8 cells (Ca^{2+} + Mg^{2+}) or 15 cells (Ba^{2+} + Mg^{2+}).

study on gating of α1G (Serrano et al., 1999) and other reports on Ca^{2+}/Na^+ selectivity of T-channels (Fukushima and Hagiwara, 1985). V_R is less positive than commonly observed for calcium currents in native cells because most such studies use Cs^+ (or even less permeant ions such as *N*-methyl-D-glucamine) to improve current isolation, and calcium channels are ~3-fold selective for Na^+ over Cs^+ (Fukushima and Hagiwara, 1985; Lux et al., 1990; Hess et al., 1986; Dashti et al., 1999). We found it convenient to use Na_i^+ because outward currents and V_R were easily measurable, and the presence of a single permeant monovalent cation simplified calculation of permeability ratios (Eq. 1).

The instantaneous *I-V* relations in Ca^{2+} have a sigmoidal shape, indicating a relatively high conductance at strongly negative or positive voltages, and a low conductance near the reversal potential. As for L-channels (Hess et al., 1986), this presumably indicates Ca^{2+} permeation at negative voltages, permeation of monovalent cations at positive voltages, and mutual block near the reversal potential.

When Ca^{2+} was replaced by Ba^{2+}, the instantaneous *I-V* was affected in several ways. V_R was 7 mV less positive (+18.8 ± 2.1 mV, $n = 15$; $p = 0.03$), outward currents were ~2-fold larger, and inward currents were ~3-fold smaller. The shift in V_R is consistent with the idea that the channel pore binds Ca^{2+} more tightly than Ba^{2+}, as for L-channels. Weaker binding of Ba^{2+} could also explain the larger outward Na^+ currents. However, the considerably smaller inward currents with Ba^{2+} were a surprise, as currents through L-channels are larger for Ba^{2+} than Ca^{2+} (Hess and Tsien, 1984), and most T-channels exhibit similar inward currents with Ca^{2+} and Ba^{2+} (Fukushima and Hagiwara, 1985; Carbone and Lux, 1987). Even for α1G, some other studies have found comparable currents with Ca^{2+} and Ba^{2+} (Klugbauer et al., 1999; Monteil et al., 2000). We suspected that this discrepancy resulted from some difference in recording conditions. The weak voltage-dependence of the inward currents in Ba^{2+}, reminiscent of voltage-dependent block, focused our attention on Mg_o^{2+}, a known blocker of calcium channels (Wilson et al., 1983; Kuo and Hess, 1993), including T-channels (Fukushima and Hagiwara, 1985; Lux et al., 1990).

Mg_o^{2+} selectively blocks inward currents carried by Ba^{2+}

One millimolar Mg_o^{2+} strongly blocked inward currents carried by 2 mM Ba^{2+} (Fig. 2). Interestingly, outward currents (carried by Na^+) were not affected. Averaging across cells, the ratio of currents with/without Mg_o^{2+} was 0.19 ± 0.04 at −120 mV ($p = 1 \times 10^{-6}$), but 1.03 ± 0.22 at +60 mV (n.s.). Because Mg^{2+} blocks T-currents more potently with monovalents as charge carrier (Fukushima and Hagiwara, 1985), the preferential block of inward currents presumably reflects voltage-dependent block (analyzed further below). Note that the *I-V* relations measured by this protocol would not be affected by effects of Mg^{2+} on channel gating, e.g., by screening of surface charge.

Mg_o^{2+} also blocked currents carried by 2 mM Ca^{2+}, but more weakly (Fig. 3). Current ratios (with/without 1 mM Mg_o^{2+}) were 0.62 ± 0.15 at −120 mV ($p = 0.04$), and 1.15 ± 0.24 at +60 mV (n.s.). In an attempt to match the degree of block observed with Ba^{2+}, the effect of 6 mM Mg_o^{2+} was tested on currents with 2 mM Ca^{2+} (Fig. 4).

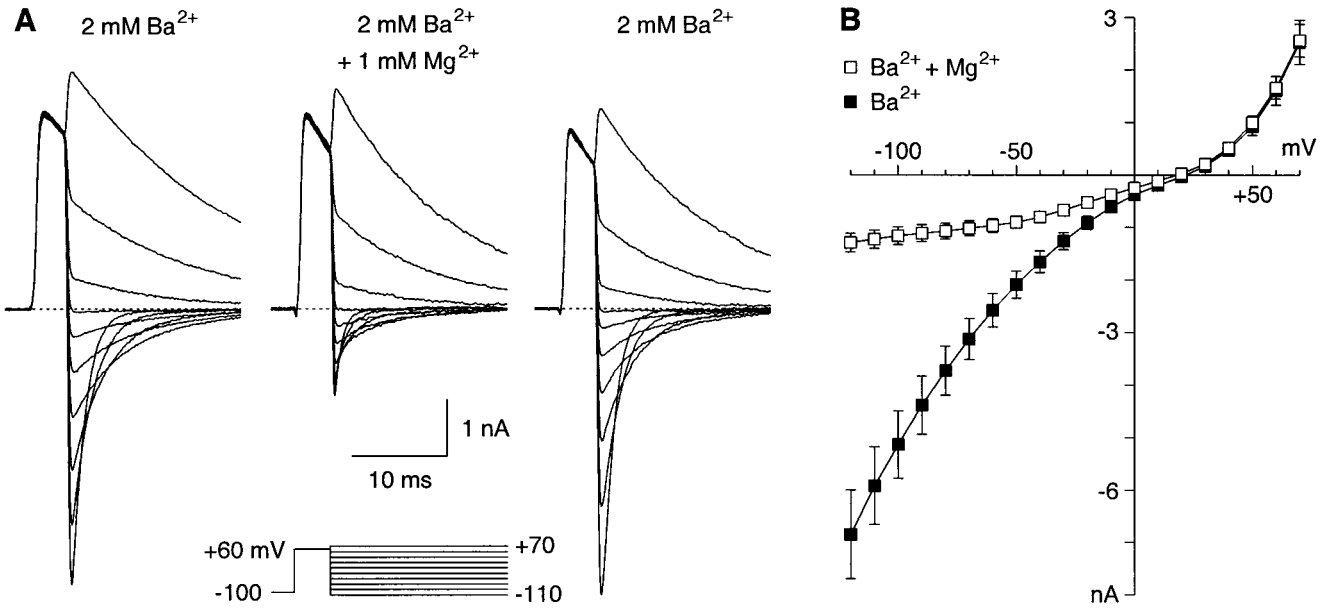

FIGURE 2 One millimolar Mg^{2+} strongly blocks inward currents with Ba^{2+}. (*A*) Sample records from one cell (a0130), recorded before (*left*), during (*middle*), and after recovery (*right*) from application of 1 mM Mg^{2+}. Note that Mg^{2+} reversibly inhibited inward currents with no effect on outward currents. The prepulse (4 ms) was twice the duration normally used, so more inactivation occurred during the prepulse. (*B*) Instantaneous *I-V* relations, averaged from 13 cells (Ba^{2+}) or 15 cells (Ba^{2+} + Mg^{2+}).

Current ratios were 0.23 ± 0.04 at −120 mV ($p = 4 \times 10^{-6}$), and 0.75 ± 0.14 at +60 mV (n.s.). Mg^{2+} had no significant effect on V_R, either with Ca^{2+} or with Ba^{2+}.

In the absence of Mg_o^{2+}, inward currents were very similar with Ca^{2+} or Ba^{2+} (Fig. 5). This confirms that nearly all of the difference in inward currents in Fig. 1 can be attributed to selective Mg^{2+} block of currents carried by Ba^{2+}. However, two subtle but important differences remain between the *I-V* relations in Ca^{2+} and Ba^{2+}. The outward currents are smaller in Ca^{2+} (Ca^{2+}/Ba^{2+} ratio 0.47 ± 0.09

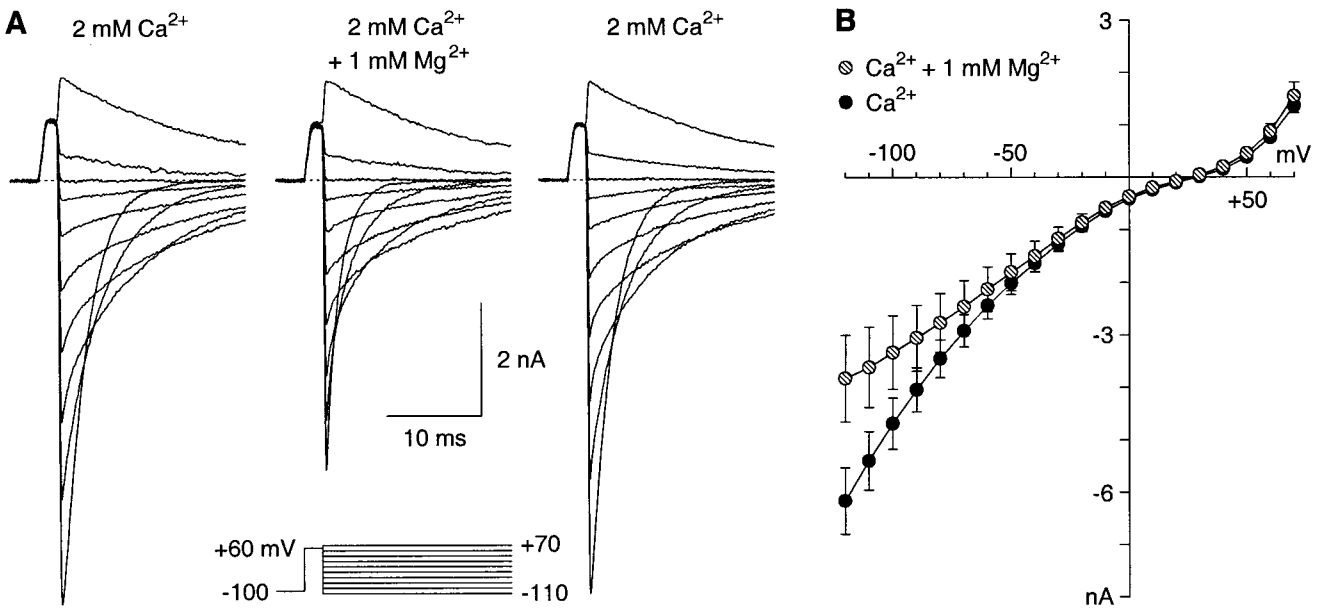

FIGURE 3 One millimolar Mg^{2+} weakly blocks inward currents with Ca^{2+}. (*A*) Sample records, cell g0209. (*B*) Instantaneous *I-V* relations, averaged from 17 cells (Ca^{2+}) or 8 cells (Ca^{2+} + Mg^{2+}).

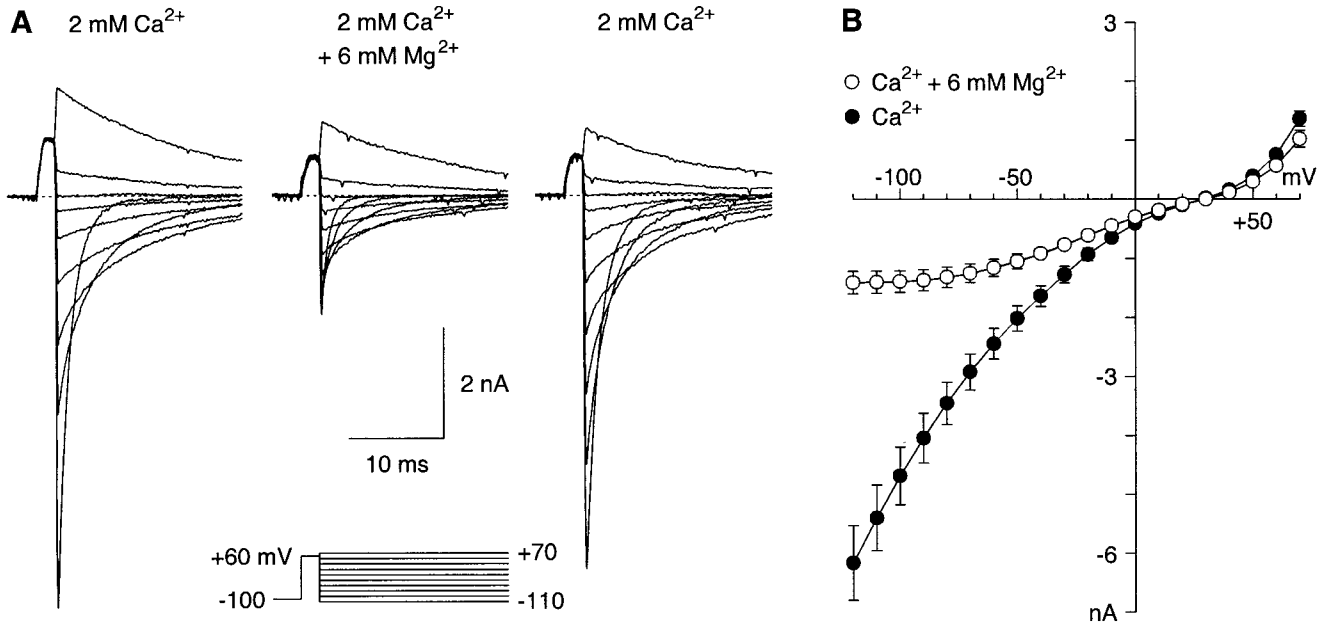

FIGURE 4 Six millimolar Mg^{2+} strongly blocks inward currents with Ca^{2+}. (*A*) Sample records, cell x0303. (*B*) Instantaneous *I-V* relations, averaged from 17 cells (Ca^{2+}) and 11 cells (Ca^{2+} + Mg^{2+}).

at +60 mV, $p = 0.003$; versus 0.90 ± 0.15 at −120 mV, n.s.), and V_R is more positive in Ca^{2+} (+28.9 ± 1.3 mV in Ca^{2+}, $n = 18$; +23.0 ± 2.1 mV in Ba^{2+}, $n = 13$; $p = 0.02$). In terms of Goldman-Hodgkin-Katz theory, these V_R values correspond to $P_{Ca}/P_{Na} = 193$, and $P_{Ba}/P_{Na} = 115$ (Eq. 1).

Like most T-channels, α1G passes similar inward currents with Ca^{2+} and Ba^{2+} (in the absence of Mg_o^{2+}). However, that does not mean that the α1G channel cannot distinguish Ca^{2+} from Ba^{2+}. Three observations indicate that the α1G pore interacts more strongly with Ca^{2+} than

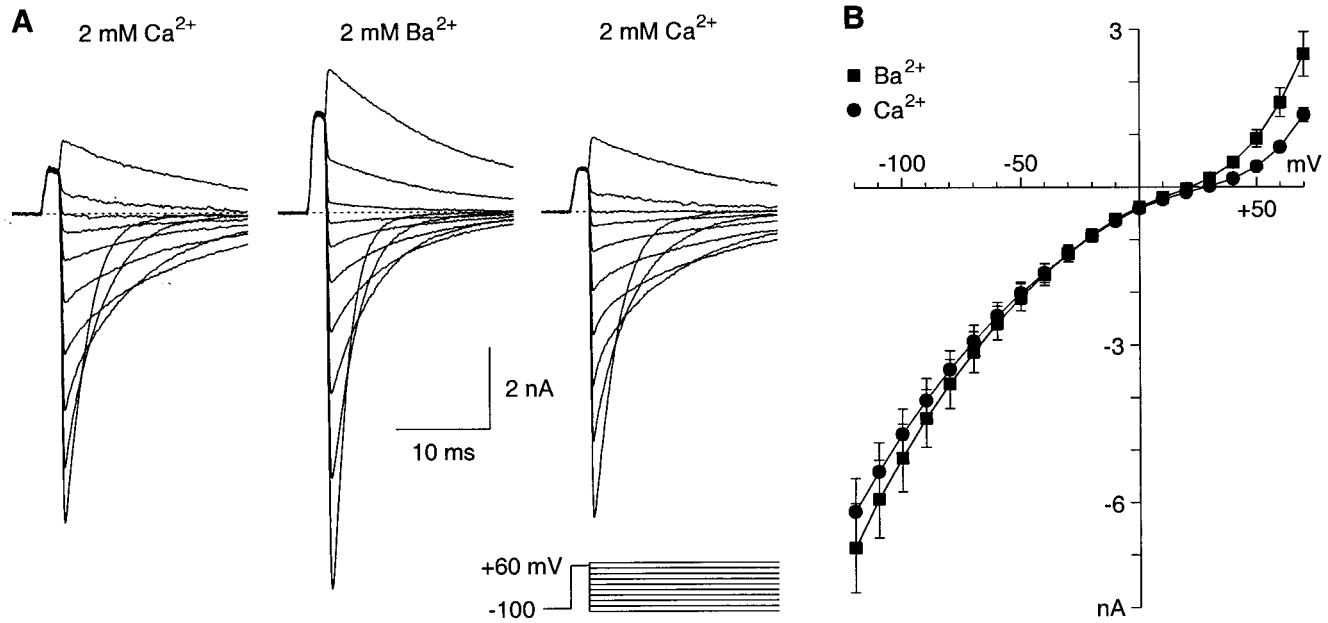

FIGURE 5 Without Mg^{2+}, inward currents are comparable with Ca^{2+} or Ba^{2+}. (*A*) Sample records, from the same cell as Fig. 3 *A*. (*B*) Instantaneous *I-V* relations, averaged from 17 cells (Ca^{2+}) or 13 cells (Ba^{2+}).

with Ba^{2+}: the permeability ratio is larger with Ca^{2+}, outward currents are smaller with Ca^{2+} (indicating stronger block of Na^+ currents by Ca^{2+}), and Ba^{2+} currents are blocked more potently by Mg^{2+}.

Mg_i^{2+} does not block strongly

Our standard recording solutions included 4 mM MgATP, estimated to produce 0.8 mM free Mg_i^{2+} (see Materials and Methods). Because a comparable concentration of Mg_o^{2+} potently blocked currents with Ba^{2+}, we examined the effect of removing Mg_i^{2+} by dialyzing cells without MgATP (and including 1 mM EDTA). No significant difference was observed in the instantaneous *I-V* relationship, although there was a suggestion of larger outward currents in the absence of Mg_i^{2+} (Fig. 6). Although we cannot exclude a weak blocking effect of Mg_i^{2+}, block by Mg^{2+} is clearly stronger from the extracellular side of the channel, as reported previously for L-channels (Kuo and Hess, 1993).

Effects on channel kinetics

The description of Mg^{2+} block presented so far effectively assumes that Mg^{2+} block is instantaneous with respect to the speed of our voltage clamp. Clearly, the strong block of the peak inward tail currents in Fig. 2 *A* and Fig. 4 *A* demonstrates that Mg^{2+} can block α1G channels rapidly. However, in several cells, especially when the clamp quality was judged to be especially good, there was a fast component to the tail currents in the presence of 2 mM Ba^{2+} + 1 mM Mg^{2+} (*arrow*, Fig. 7 *B*). That component is not a residual capacity transient or a gating current, because 1) it is not seen in the absence of Mg^{2+} (Fig. 7 *A*), 2) it is greatly reduced by partial inactivation (Fig. 7 *B*), and 3) it is absent in 10 mM Mg^{2+} (Fig. 7 *C*), where block should be 10-fold faster. We interpret that rapid component as the partially resolved time course of Mg^{2+} block. Our method of measuring the instantaneous *I-V* relationship was designed to avoid including the fast component (see Materials and Methods). Thus, the measured currents should reflect the extent of block at each voltage following equilibration of Mg^{2+} with the open channel. There was no obvious fast component to tails with Ca^{2+} + Mg^{2+}, probably because the extent of block was low with 1 mM Mg^{2+}, and the rate of block was high with 6 mM Mg^{2+}.

Our results suggest that the time constant for block by 1 mM Mg^{2+} is ~0.1 ms, possibly faster. That would correspond to a bimolecular blocking rate of $\sim 10^7\ M^{-1}\ s^{-1}$. For comparison, for high voltage-activated (HVA) calcium channels, Mg^{2+} blocks currents carried by monovalent cations at $\sim 10^8\ M^{-1}\ s^{-1}$ (Kuo and Hess, 1993; Carbone et al., 1997). With 110 mM Ba^{2+}, the rate is $1.9 \times 10^5\ s^{-1}$, but that increases sharply at lower Ba^{2+} (Lansman et al., 1986).

Although our experiments were designed to analyze effects on permeation, preliminary results suggest that Mg^{2+} may also affect gating. With a "standard *I-V*" protocol, where the cell was depolarized directly to a range of voltages without a prepulse to +60 mV, Mg^{2+} appeared to shift

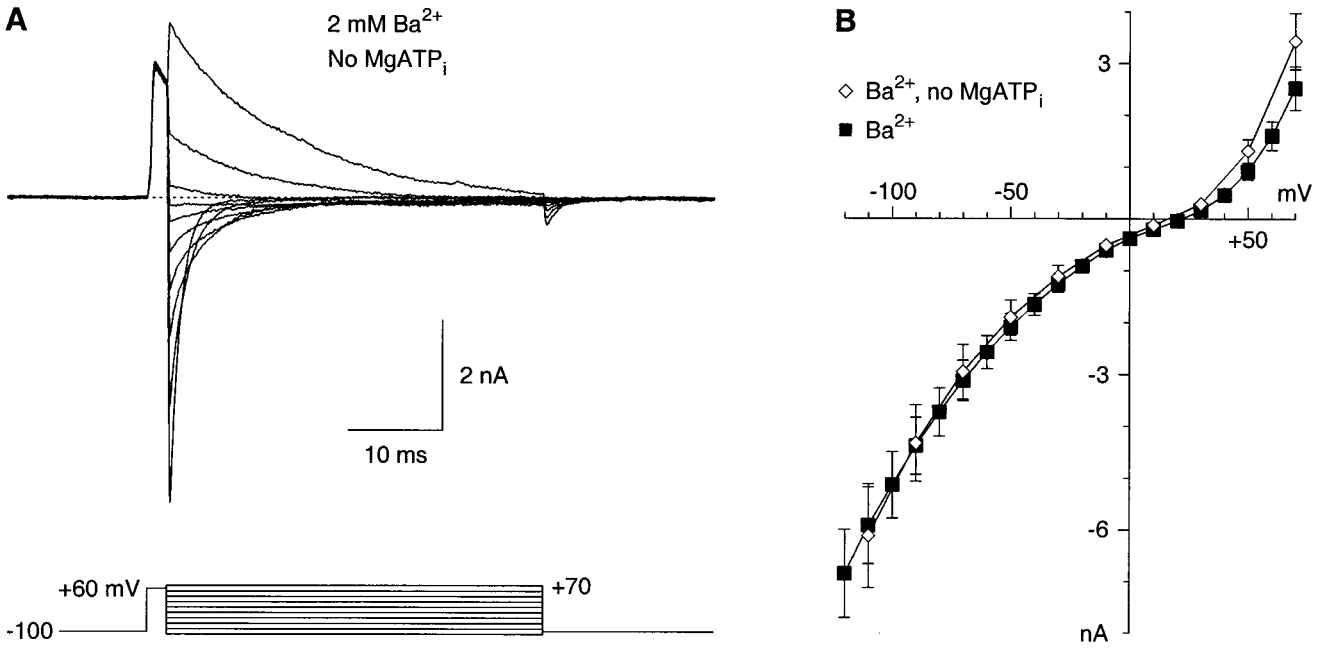

FIGURE 6 Mg_i^{2+} has little or no effect. (*A*) Sample records from a cell (b9728) dialyzed with an intracellular solution containing 1 mM EDTA and no MgATP. (*B*) Instantaneous *I-V* relations, averaged from 8 cells (Ba^{2+}, no MgATP) or 13 cells (Ba^{2+}).

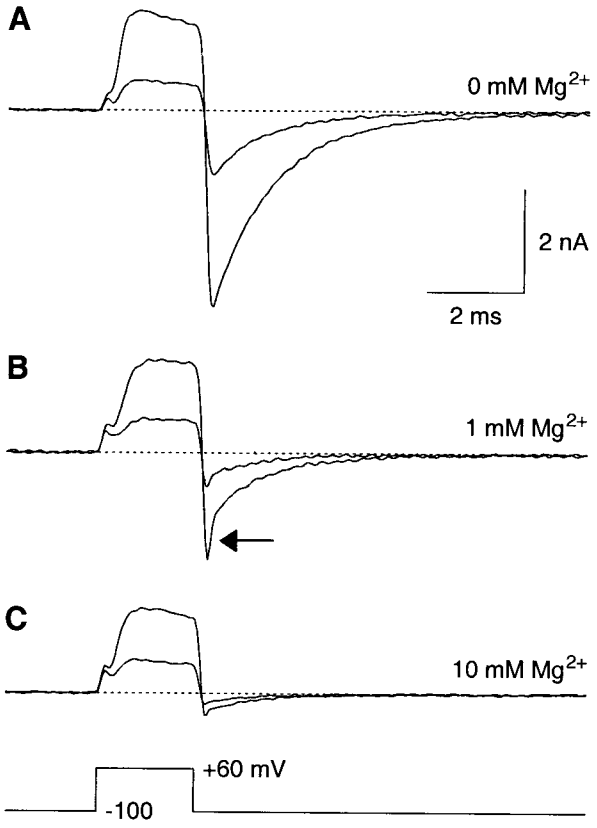

FIGURE 7 A fast component to inward tail currents in 2 mM Ba^{2+} + 1 mM Mg^{2+}. Currents were recorded in response to 2-ms steps to +60 mV, in the absence of Mg_o^{2+} (*A*), with 1 mM Mg_o^{2+} (*B*), or with 10 mM Mg_o^{2+} (*C*). In each condition two records are shown, one in a rested cell (the larger current), and one following partial inactivation (by a 42-ms step to +60 mV, followed by 20 ms at −120 mV to allow channels to deactivate fully). Same cell as Fig. 6 *A* (no intracellular MgATP). Similar fast tail current components could also be observed in cells with MgATP; 2.5 kHz Gaussian filter.

channel gating by ~10 mV to more depolarized voltages (data not shown). Consequently, at negative voltages, the percentage inhibition by Mg^{2+} was greater measured from the standard *I-V* than from the "instantaneous *I-V*." With Ca^{2+}, addition of either 1 or 6 mM Mg^{2+} decreased the time constants for channel deactivation; the effect of Mg^{2+} on the main component of deactivation was less clear with Ba^{2+}. These effects are in the direction expected for screening by Mg^{2+} of a surface charge associated with gating, but we cannot rule out additional effects (e.g., altered activation of a Mg^{2+}-blocked channel, or modification of gating by binding of Mg^{2+} to a separate site outside the pore). Mg^{2+} did not affect the time constant for inactivation, but inactivation of inward currents was ~30% faster in Ba^{2+} than in Ca^{2+}, as previously reported for α1G (Klugbauer et al., 1999).

For purposes of this paper, we conclude that our measurements of instantaneous *I-V* relations reflect the voltage-dependence of Mg^{2+} block of the open channel, with negligible interference from effects on gating, or time-dependence of Mg^{2+} block. Possible effects of Mg^{2+} and other blockers on gating of α1G (Lee et al., 1999b; Lacinová et al., 2000) will require further study.

Analysis of Mg^{2+} block

Block by Mg^{2+} is clearly voltage-dependent (Figs. 2–4). We first examined whether the voltage-dependence was consistent with a simple Woodhull model (Eq. 2), where Mg^{2+} can enter and exit the pore only from the extracellular side (Fig. 8). The data were fitted reasonably well, especially for Ca^{2+}, assuming a binding site 25–30% of the distance through the electrical field of the membrane from the outside, with 7-fold lower affinity with Ca^{2+} as the charge carrier.

The lower affinity for Mg^{2+} in the presence of Ca^{2+} presumably reflects ion-ion competition, not considered in a Woodhull model. We next tested Eyring rate theory models, including two binding sites within the channel pore, based on the classical models for permeation and block of L-

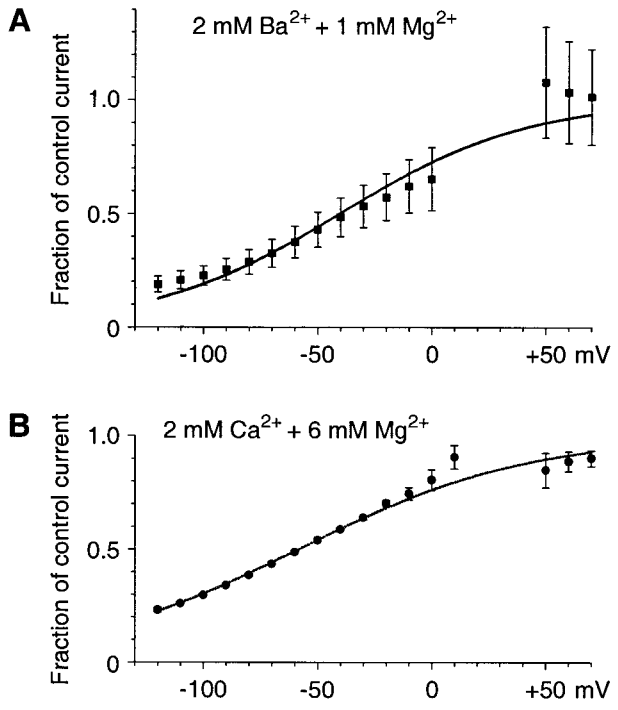

FIGURE 8 Analysis of Mg^{2+} block using a Woodhull model. (*A*) The current ratio (Ba^{2+} + Mg^{2+}/Ba^{2+}) calculated from the data of Fig. 2 *B*. The smooth curve was fitted using Eq. 2, with $K_{D,0}$ = 2.7 mM and δ = 0.30. (*B*) Current ratios calculated from three cells where 6 mM Mg^{2+} reversibly inhibited the currents with 2 mM Ca^{2+}. The average of currents recorded before and after recovery from Mg^{2+} block was used as the control. Because the comparisons were made within each cell rather than across populations of cells, the standard errors are less in *B* than in *A*. The fit to Eq. 2 gave $K_{D,0}$ = 19 mM and δ = 0.25 (*smooth curve*).

channels (Almers and McCleskey, 1984; Hess and Tsien, 1984). The best-fit parameters reproduced many of the key features of the data, in five experimental conditions (Ca^{2+} alone, Ba^{2+} alone, Ca^{2+} or Ba^{2+} + 1 mM Mg^{2+}, and Ca^{2+} + 6 mM Mg^{2+}), over a 190 mV range: the overall shape of the *I-V* relations, similar inward currents with Ca^{2+} or Ba^{2+} (in the absence of Mg^{2+}), stronger block of inward currents carried by Ba^{2+}, a more positive reversal potential with Ca^{2+}, and larger outward currents with Ba^{2+} (Fig. 9). The parameters produced Ca^{2+}/Ba^{2+} selectivity using deeper wells for Ca^{2+} (higher affinity binding), but higher barriers for Ba^{2+} (slower entry into the pore). Both differences contribute to the more positive reversal potential with Ca^{2+}, but the effects on the amplitudes of inward currents are opposite and nearly cancel. Crudely put, Ca^{2+} can get into the pore more easily than Ba^{2+}, but once in, it is less likely to exit. The energy differences are quite small, so it is striking that the model reproduces the ~7-fold difference in Mg^{2+} block. Both differences between the energetics of Ca^{2+} and Ba^{2+} favor Ca^{2+} occupancy, reducing the ability of Mg^{2+} to enter and block.

The Eyring model predicts that Na^+ carries an appreciable fraction of the inward current, even in the presence of 2 mM Ca^{2+} or Ba^{2+}. At −50 mV, Na^+ would carry 18% of the current with Ca^{2+}, and 50% with Ba^{2+}; the fractional Na^+ current would increase with hyperpolarization (calculations not shown). Because the net currents are nearly equal with 2 mM Ca^{2+} or Ba^{2+} (in the absence of Mg_o^{2+}), there actually would be more Ca^{2+} entry than Ba^{2+} entry. It is not clear whether this feature of the model is realistic.

For the Eyring model, the energy profile for Mg^{2+} includes a high energy barrier on the cytoplasmic side of the channel. That explains why a Woodhull model (effectively assuming an infinitely high barrier) can describe Mg^{2+} block reasonably well. The high barrier also explains the asymmetry in Mg^{2+} block, where Mg_o^{2+} blocks potently while Mg_i^{2+} does not. For Mg^{2+}, the outer site was not well defined, and in practical terms is not really a binding site.

It is interesting that the Woodhull models suggested that Mg^{2+} bound toward the outer part of the channel (δ = 0.25–0.30), while the Eyring model placed the site of Mg^{2+} block toward the cytoplasmic side (δ = 0.67). When the output of the Eyring model was fitted to a Woodhull model (Eq. 2), the fits were less good than in Fig. 8, with δ values for Mg^{2+} of 0.23 (with Ca^{2+}) and 0.29 (with Ba^{2+}). This illustrates that that Woodhull parameters cannot be interpreted literally for a multi-ion pore (Hille, 1992). We have not systematically varied the position of the binding sites in the Eyring model, so the δ = 0.67 value should not be taken too literally. However, if the binding sites were constrained to be in the outer part of the channel (δ = 0.2 and 0.3) (see Kuo and Hess, 1993), we were not able to obtain a good fit to the data (calculations not shown).

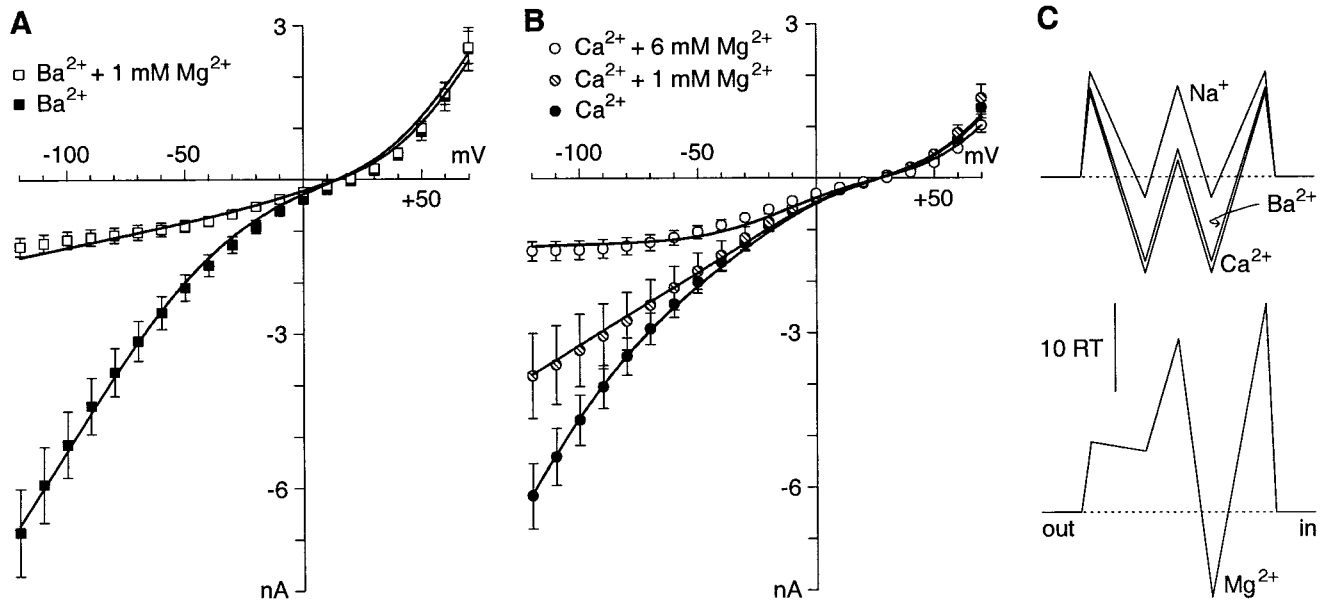

FIGURE 9 Analysis of Mg^{2+} block using an Eyring rate theory model. (*A* and *B*) The smooth curves are the best fits to a 2-site, 3-barrier model, superimposed on the experimental data from Fig. 2 *B* and Fig. 3 *B*, respectively. The model-generated single-channel currents were scaled to match the whole-cell currents, assuming 8000 open channels. (*C*) The energy profiles for the different ions. The model was based on that of Almers and McCleskey (1984); see Materials and Methods for details. The energy barriers and wells (from outside to inside) were 9.62, −10.91, 1.87, −10.91, 9.62 (Ca^{2+}); 10.17, −9.60, 3.17, −9.60, 10.17 (Ba^{2+}); 12, −2.38, 10.39, −2.38, 12 (Na^+); and 8, 7, 19.77, −9.75, 23.75 (Mg^{2+}). In the format recommended by the Journal of General Physiology (Andersen, 1999), 10 *RT* corresponds to RCR = 4.3, assuming a frequency factor of 6.1×10^{12} (see Materials and Methods).

Recently, many crucial features of L-channel permeation have been described by a different theoretical approach, Poisson-Nernst-Planck (PNP) theory (Nonner and Eisenberg, 1998). PNP can qualitatively reproduce several of our principal results if we assume that the chemical potential for Mg^{2+} varies linearly within the pore (to explain the asymmetrical block; calculations not shown). However, we have not found parameters that quantitatively describe the instantaneous *I-V* curves. Thus far, we have attempted to find appropriate PNP parameters "by hand" rather than by automated error-minimization routines (as used above for Eyring models), so we cannot conclude that PNP theory is unable to explain our results.

DISCUSSION

Although Ca^{2+} and Ba^{2+} carry comparable inward currents through the α1G T-type calcium channel, the channel is actually selective for Ca^{2+} over Ba^{2+}. This difference is shown most clearly by the ~7-fold difference in the apparent affinity for block by Mg^{2+}. A more positive reversal potential with Ca^{2+}, and stronger block of outward currents by Ca^{2+}, also imply that Ca^{2+} interacts more strongly with the α1G pore than does Ba^{2+}. In terms of an Eyring rate theory model, Ca^{2+} enters the pore more easily than Ba^{2+}, but exits more slowly.

Ca^{2+}-Ba^{2+} selectivity

Most studies on native T-type calcium channels found similar inward currents with Ca^{2+} and Ba^{2+} (Huguenard, 1996), with the exception of thalamic reticular neurons, where Ca^{2+} currents were ~50% larger (Huguenard and Prince, 1992). However, comparison among studies can be difficult. The Ca^{2+} and Ba^{2+} concentrations have varied from the physiological range to isotonic (especially for single-channel studies), which could affect the apparent selectivity. Many studies used the current at the peak of the *I-V* relationship as an index, which could be affected by changes in channel gating as well as by the conductance of the channel to Ca^{2+} or Ba^{2+}. The activation of L-type and other HVA channels is known to be affected by surface potentials, which can differ between Ca^{2+} and Ba^{2+} even at the same concentration; few studies have examined effects of surface potential on T-channels (Becchetti et al., 1992).

Few studies of T-currents have compared reversal potentials or outward currents for Ca^{2+} versus Ba^{2+}. One important exception is Fukushima and Hagiwara (1985), who found for T-currents of B lymphocytes that the reversal potential was ~10 mV more positive and outward currents were smaller with Ca^{2+}, in good agreement with our results for α1G.

One of our main conclusions is that α1G T-channels resemble L-channels in selectivity for Ca^{2+} over Ba^{2+}, by traditional criteria such as permeability ratios. For L-channels, the channel conductance is higher for Ba^{2+} (opposite to the selectivity sequence), while for α1G the whole-cell Ca^{2+} and Ba^{2+} conductances are similar. In terms of an Eyring model, in L-channels the primary difference in energy profiles for Ca^{2+} and Ba^{2+} is a deeper energy well for Ca^{2+} by ~4 *RT* (Almers and McCleskey, 1984). For α1G, our parameters also give a deeper well for Ca^{2+}, but only by 1.3 *RT*. We also found a lower external barrier for Ca^{2+} not present in the L-channel models. Overall, it is noteworthy that relatively modest differences in energy profiles can have significant effects on ion selectivity and block.

Calcium channels often show an anomalous mole fraction effect (AMFE) between Ca^{2+} and Ba^{2+}, where the current in a mixture of Ca^{2+} and Ba^{2+} is less than with either ion alone (Almers and McCleskey, 1984; Hess and Tsien, 1984). The Eyring model predicts a very weak AMFE for α1G, maximally a 6% reduction in current amplitudes near −60 mV, and no AMFE for the reversal potential (calculations not shown).

Although the Eyring model for α1G gave a good quantitative description of our results, we emphasize the qualitative explanation that it provides for the differential sensitivity of Ca^{2+} and Ba^{2+} currents to Mg^{2+} block. First, the results presented here are limited to a single concentration (2 mM) of divalent cation as charge carrier. Preliminary results demonstrate substantial increases in current either upon removal of extracellular divalent cations (and addition of EGTA), or in isotonic Ca^{2+} or Ba^{2+}, but those data are not yet suitable for quantitative modeling. Second, there is a lively debate regarding the physical plausibility of Eyring models for channel permeation (McCleskey, 1999; Nonner et al., 1999). One specific issue is that Eyring models (including ours) tend to predict significant changes in the net charge in the pore with voltage and ion concentration, while PNP models predict an essentially electroneutral pore (Nonner and Eisenberg, 1998). For the moment, we present this model as one specific and intuitive explanation of interactions among Ca^{2+}, Ba^{2+}, and Mg^{2+}.

The molecular basis for the variations in selectivity among calcium channels remains to be explored. All known HVA channels contain four glutamates in the P region, at the corresponding site in each of the four P loops, and mutations at those sites strongly affect channel selectivity (Yang et al., 1993). The cloned T-channels contain aspartates at two of those positions, in domains III and IV (Perez-Reyes et al., 1998; Cribbs et al., 1998; Lee et al., 1999a). Those differences are an obvious candidate for the changes in selectivity (Yang et al., 1999), but are unlikely to explain all differences in selectivity and block among calcium channels. For example, the α1E channel, which has four glutamates, exhibits larger currents with Ca^{2+} than with Ba^{2+} (Bourinet et al., 1996). Also, the α1H T-channel is ~20-fold more sensitive to block by Ni^{2+} than are the other cloned T-channels (Lee et al., 1999b).

Mg^{2+} block

Although Mg^{2+} block of calcium channels is well established, we were surprised by the potency of the block, which appears to be stronger than for L-type channels (Campbell et al., 1988; Hartzell and White, 1989; Wu and Lipsius, 1990; Dichtl and Vierling, 1991; Hall and Fry, 1992; Zhang et al., 1995; Song et al., 1996), although the use of different charge carriers at different concentrations again makes direct comparisons difficult. In cardiac cells, one study also found that Mg^{2+} inhibited T-channels more effectively than L-channels (Wu and Lipsius, 1990). For N-type channels of frog sympathetic neurons, with 2 mM Ba^{2+}, the effect of 3 mM Mg^{2+} on the instantaneous *I-V* relationship could be described by a Woodhull model with $\delta = 0.25$ and $K_{D,0} = 9$ mM (W. Zhou and S. W. Jones, unpublished observations), ~3-fold weaker block than found here for α1G.

It has been suggested that Mg^{2+} "block" actually results from screening of surface charge, rather than true pore block (Wilson et al., 1983). Although we do not have an estimate for the surface charge associated with T-channels, it is unlikely that a surface charge-mediated effect of 1 mM Mg^{2+} (in the presence of 2 mM Ba^{2+}) could be as strong and as voltage-dependent as observed (Fig. 2 *B*). Furthermore, there is evidence (at least for HVA channels) that little surface charge is associated with permeation, in contrast to the well-known effects of surface charge on gating (Kuo and Hess, 1993; Zhou and Jones, 1995). The observation of discrete Mg^{2+} block of single L-channels also argues against a surface charge mechanism (Lansman et al., 1986; Kuo and Hess, 1993).

It is well known that blockade of calcium channels is a competitive process that depends on the nature and concentration of permeant ion (Hagiwara et al., 1974; Hess and Tsien, 1984; Lansman et al., 1986; Yang et al., 1993). In the calcium channel of barnacle muscle, Ba^{2+} normally carries larger currents than Ca^{2+}, but currents are larger with Ca^{2+} following partial blockade by Co^{2+}, early evidence that ion selectivity in calcium channels involves selective binding (Hagiwara et al., 1974). Similarly, currents carried by Ba^{2+} are more sensitive to block by Mg^{2+} in cardiac L-channels (Campbell et al., 1988). For α1G, one recent study noted that block by Cd^{2+} and Ni^{2+} is more potent with Ba^{2+} than with Ca^{2+} (Lacinová et al., 2000).

Although we have emphasized mechanistic implications, Mg^{2+} block of T-current may also play a physiological or pharmacological role. Even with Ca^{2+}, 1 mM Mg^{2+} produced a modest inhibition of inward current, suggesting that Mg^{2+} block occurs even under physiological conditions. The block is stronger at more negative voltages, where significant Ca^{2+} entry can occur through T-channels during the "tail current" following an action potential (Huguenard, 1996). In cardiac cells, Mg^{2+} block of T-current has been suggested to play a role in the antiarrhythmic effect of elevated Mg_o^{2+} (Wu and Lipsius, 1990).

As a practical matter, our results demonstrate that the choice of $[Mg^{2+}]_o$ can critically affect the outcome of experiments on calcium channels in vitro. Furthermore, Mg^{2+} block can be a useful tool for dissection of calcium channel selectivity.

We thank Eric G. George for programming Poisson-Nernst-Planck models.

This work was supported in part by National Institutes of Health Grants NS24471 (to S.W.J.) and NS38691 (to E.P.-R.), and by a Howard Hughes Medical Institute grant to Case Western Reserve University School of Medicine.

REFERENCES

Almers, W., and E. W. McCleskey. 1984. Non-selective conductance in calcium channels of frog muscle: calcium selectivity in a single-file pore. *J. Physiol. (Lond.).* 353:585–608.

Andersen, O. S. 1999. Editorial: Graphic representation of the results of kinetic analyses. *J. Gen. Physiol.* 114:589–590.

Bean, B. P. 1985. Two kinds of calcium channels in canine atrial cells. Differences in kinetics, selectivity, and pharmacology. *J. Gen. Physiol.* 86:1–30.

Becchetti, A., A. Arcangeli, M. R. Del Bene, M. Olivotto, and E. Wanke. 1992. Intra and extracellular surface charges near Ca^{2+} channels in neurons and neuroblastoma cells. *Biophys. J.* 63:954–965.

Bourinet, E., G. W. Zamponi, A. Stea, T. W. Soong, B. A. Lewis, L. P. Jones, D. T. Yue, and T. P. Snutch. 1996. The α_{1E} calcium channel exhibits permeation properties similar to low-voltage-activated calcium channels. *J. Neurosci.* 16:4983–4993.

Brooks, S. P., and K. B. Storey. 1992. Bound and determined: a computer program for making buffers of defined ion concentrations. *Anal. Biochem.* 201:119–126.

Campbell, D. L., W. R. Giles, and E. F. Shibata. 1988. Ion transfer characteristics of the calcium current in bull-frog atrial myocytes. *J. Physiol. (Lond.).* 403:239–266.

Carbone, E., and H. D. Lux. 1987. Kinetics and selectivity of a low-voltage-activated calcium current in chick and rat sensory neurones. *J. Physiol. (Lond.).* 386:547–570.

Carbone, E., H. D. Lux, V. Carabelli, G. Aicardi, and H. Zucker. 1997. Ca^{2+} and Na^{+} permeability of high-threshold Ca^{2+} channels and their voltage-dependent block by Mg^{2+} ions in chick sensory neurones. *J. Physiol. (Lond.).* 504:1–15.

Cribbs, L. L., J. H. Lee, J. Yang, J. Satin, Y. Zhang, A. Daud, J. Barclay, M. P. Williamson, M. Fox, M. Rees, and E. Perez-Reyes. 1998. Cloning and characterization of α1H from human heart, a member of the T-type Ca^{2+} channel gene family. *Circ. Res.* 83:103–109.

Dang, T. X., and E. W. McCleskey. 1998. Ion channel selectivity through stepwise changes in binding affinity. *J. Gen. Physiol.* 111:185–193.

Dashti, S. R., J. R. Serrano, L. L. Cribbs, E. Perez-Reyes, and S. W. Jones. 1999. Selectivity of the α_{1G} T-type Ca^{2+} channel. *Biophys. J.* 76:409*a*. (Abstr.).

Dichtl, A., and W. Vierling. 1991. Inhibition by magnesium of calcium inward current in heart ventricular muscle. *Eur. J. Pharmacol.* 204: 243–248.

Frazier, C. J., E. G. George, and S. W. Jones. 2000. Apparent change in ion selectivity caused by changes in intracellular K^{+} during whole-cell recording. *Biophys. J.* 78:1872–1880.

Fukushima, Y., and S. Hagiwara. 1985. Currents carried by monovalent cations through calcium channels in mouse neoplastic B lymphocytes. *J. Physiol. (Lond.).* 358:255–284.

Hagiwara, S., J. Fukuda, and D. C. Eaton. 1974. Membrane currents carried by Ca, Sr, and Ba in barnacle muscle fiber during voltage clamp. *J. Gen. Physiol.* 63:564–578.

Hall, S. K., and C. H. Fry. 1992. Magnesium affects excitation, conduction, and contraction of isolated mammalian cardiac muscle. *Am. J. Physiol. Heart Circ. Physiol.* 263:H622–H633.

Hartzell, H. C., and R. E. White. 1989. Effects of magnesium on inactivation of the voltage-gated calcium current in cardiac myocytes. *J. Gen. Physiol.* 94:745–767.

Hess, P., J. B. Lansman, and R. W. Tsien. 1986. Calcium channel selectivity for divalent and monovalent cations. Voltage and concentration dependence of single channel current in ventricular heart cells. *J. Gen. Physiol.* 88:293–319.

Hess, P., and R. W. Tsien. 1984. Mechanism of ion permeation through calcium channels. *Nature.* 309:453–456.

Hille, B. 1992. Ionic Channels of Excitable Membranes, 2nd Ed. Sinauer Associates, Sunderland, MA.

Hodgkin, A. L., and A. F. Huxley. 1952. The components of membrane conductance in the giant axon of *Loligo. J. Physiol. (Lond.).* 116: 473–496.

Huguenard, J. R. 1996. Low-threshold calcium currents in central nervous system neurons. *Annu. Rev. Physiol.* 58:329–348.

Huguenard, J. R., and D. A. Prince. 1992. A novel T-type current underlies prolonged Ca^{2+}-dependent burst firing in GABAergic neurons of rat thalamic reticular nucleus. *J. Neurosci.* 12:3804–3817.

Klugbauer, N., E. Marais, L. Lacinova, and F. Hofmann. 1999. A T-type calcium channel from mouse brain. *Pflugers Arch.* 437:710–715.

Kuo, C. C., and P. Hess. 1993. Block of the L-type Ca^{2+} channel pore by external and internal Mg^{2+} in rat phaeochromocytoma cells. *J. Physiol. (Lond.).* 466:683–706.

Lacinová, L., N. Klugbauer, and F. Hofmann. 2000. Regulation of the calcium channel α_{1G} subunit by divalent cations and organic blockers. *Neuropharmacology.* 39:1254–1266.

Lansman, J. B., P. Hess, and R. W. Tsien. 1986. Blockade of current through single calcium channels by Cd^{2+}, Mg^{2+}, and Ca^{2+}. Voltage and concentration dependence of calcium entry into the pore. *J. Gen. Physiol.* 88:321–347.

Lee, J.-H., A. N. Daud, L. L. Cribbs, A. E. Lacerda, A. Pereverzev, U. Klöckner, T. Schneider, and E. Perez-Reyes. 1999a. Cloning and expression of a novel member of the low voltage-activated T-type calcium channel family. *J. Neurosci.* 19:1912–1921.

Lee, J.-H., J. C. Gomora, L. L. Cribbs, and E. Perez-Reyes. 1999b. Nickel block of three cloned T-type calcium channels: low concentrations selectively block α1H. *Biophys. J.* 77:3034–3042.

Lux, H. D., E. Carbone, and H. Zucker. 1990. Na^+ currents through low-voltage-activated Ca^{2+} channels of chick sensory neurones: block by external Ca^{2+} and Mg^{2+}. *J. Physiol. (Lond.).* 430:159–188.

McCleskey, E. W. 1999. Calcium channel permeation: A field in flux. *J. Gen. Physiol.* 113:765–772.

McCleskey, E. W., and W. Almers. 1985. The Ca channel in skeletal muscle is a large pore. *Proc. Natl. Acad. Sci. U.S.A.* 82:7149–7153.

Monteil, A., J. Chemin, E. Bourinet, G. Mennessier, P. Lory, and J. Nargeot. 2000. Molecular and functional properties of the human α_{1G} subunit that forms T-type calcium channels. *J. Biol. Chem.* 275: 6090–6100.

Nonner, W., D. P. Chen, and B. Eisenberg. 1999. Progress and prospects in permeation. *J. Gen. Physiol.* 113:773–782.

Nonner, W., and B. Eisenberg. 1998. Ion permeation and glutamate residues linked by Poisson-Nernst-Planck theory in L-type calcium channels. *Biophys. J.* 75:1287–1305.

Perez-Reyes, E., L. L. Cribbs, A. Daud, A. E. Lacerda, J. Barclay, M. P. Williamson, M. Fox, M. Rees, and J. H. Lee. 1998. Molecular characterization of a neuronal low-voltage-activated T-type calcium channel. *Nature.* 391:896–900.

Serrano, J. R., E. Perez-Reyes, and S. W. Jones. 1999. State-dependent inactivation of the α1G T-type calcium channel. *J. Gen. Physiol.* 114: 185–201.

Song, Y., Q. Y. Liu, and M. Vassalle. 1996. On the antiarrhythmic actions of magnesium in single guinea-pig ventricular myocytes. *Clin. Exp. Pharmacol. Physiol.* 23:830–838.

Talley, E. M., L. L. Cribbs, J. H. Lee, A. Daud, E. Perez-Reyes, and D. A. Bayliss. 1999. Differential distribution of three members of a gene family encoding low voltage-activated (T-type) calcium channels. *J. Neurosci.* 19:1895–1911.

Wilson, D. L., K. Morimoto, Y. Tsuda, and A. M. Brown. 1983. Interaction between calcium ions and surface charge as it relates to calcium currents. *J. Membr. Biol.* 72:117–130.

Woodhull, A. M. 1973. Ionic blockage of sodium channels in nerve. *J. Gen. Physiol.* 61:687–708.

Wu, J. Y., and S. L. Lipsius. 1990. Effects of extracellular Mg^{2+} on T- and L-type Ca^{2+} currents in single atrial myocytes. *Am. J. Physiol. Heart Circ. Physiol.* 259:H1842–H1850.

Yang, J., P. T. Ellinor, W. A. Sather, J. F. Zhang, and R. W. Tsien. 1993. Molecular determinants of Ca^{2+} selectivity and ion permeation in L-type Ca^{2+} channels. *Nature.* 366:158–161.

Yang, N., E. Perez-Reyes, R. W. Aldrich, and R. W. Tsien. 1999. Replacement of L-type Ca^{2+} channel P-region residues with divergent residues of T-type channels gives rise to small single channel conductance like T-type channels. *Biophys. J.* 76:259*a*. (Abstr.).

Yue, D. T., and E. Marban. 1990. Permeation in the dihydropyridine-sensitive calcium channel. Multi-ion occupancy but no anomalous mole-fraction effect between Ba^{2+} and Ca^{2+}. *J. Gen. Physiol.* 95:911–939.

Zhang, S., T. Sawanobori, H. Adaniya, Y. Hirano, and M. Hiraoka. 1995. Dual effects of external magnesium on action potential duration in guinea pig ventricular myocytes. *Am. J. Physiol. Heart Circ. Physiol.* 268:H2321–H2328.

Zhou, W., and S. W. Jones. 1995. Surface charge and calcium channel saturation in bullfrog sympathetic neurons. *J. Gen. Physiol.* 105: 441–462.